



**Meteorological constraints on oceanic halocarbons above the Peruvian Upwelling**

S. Fuhlbrügge et al.

# Meteorological constraints on oceanic halocarbons above the Peruvian Upwelling

S. Fuhlbrügge<sup>1</sup>, B. Quack<sup>1</sup>, E. Atlas<sup>2</sup>, A. Fiehn<sup>1</sup>, H. Hepach<sup>1</sup>, and K. Krüger<sup>3</sup>

<sup>1</sup>GEOMAR, Helmholtz Centre for Ocean Research Kiel, Kiel, Germany

<sup>2</sup>Rosenstiel School for Marine and Atmospheric Sciences, Miami, FL, USA

<sup>3</sup>University of Oslo, Oslo, Norway

Received: 23 June 2015 – Accepted: 6 July 2015 – Published: 31 July 2015

Correspondence to: K. Krüger (kirstin.krueger@geo.uio.no)

Published by Copernicus Publications on behalf of the European Geosciences Union.

Title Page

Abstract

Introduction

Conclusions

References

Tables

Figures



Back

Close

Full Screen / Esc

Printer-friendly Version

Interactive Discussion



## Abstract

Halogenated very short lived substances (VSLs) are naturally produced in the ocean and emitted to the atmosphere. Recently, oceanic upwelling regions in the tropical East Atlantic were identified as strong sources of brominated halocarbons to the atmosphere. During a cruise of R/V *METEOR* in December 2012 the oceanic sources and emissions of various halogenated trace gases and their mixing ratios in the marine atmospheric boundary layer (MABL) were investigated above the Peruvian Upwelling for the first time. This study presents novel observations of the three VSLs bromoform, dibromomethane and methyl iodide together with high resolution meteorological measurements and Lagrangian transport modelling. Although relatively low oceanic emissions were observed, except for methyl iodide, surface atmospheric abundances were elevated. Radiosonde launches during the cruise revealed a low, stable MABL and a distinct trade inversion above acting both as strong barriers for convection and trace gas transport in this region. Significant correlations between observed atmospheric VSLs abundances, sea surface temperature, relative humidity and MABL height were found. We used a simple source-loss estimate to identify the contribution of oceanic emissions to observed atmospheric concentrations which revealed that the observed marine VSLs abundances were dominated by horizontal advection below the trade inversion. The observed VSLs variations can be explained by the low emissions and their accumulation under different MABL and trade inversion conditions. This study confirms the importance of oceanic upwelling and trade wind systems on creating effective transport barriers in the lower atmosphere controlling the distribution of VSLs abundances above ocean upwelling regions.

## 1 Introduction

Short-lived halocarbons from the oceans contribute to reactive atmospheric halogens, which are involved in tropospheric and stratospheric ozone depletion, aerosol forma-

### Meteorological constraints on oceanic halocarbons above the Peruvian Upwelling

S. Fuhlbrügge et al.

Title Page

Abstract

Introduction

Conclusions

References

Tables

Figures

◀

▶

◀

▶

Back

Close

Full Screen / Esc

Printer-friendly Version

Interactive Discussion



## Meteorological constraints on oceanic halocarbons above the Peruvian Upwelling

S. Fuhlbrügge et al.

Title Page

Abstract

Introduction

Conclusions

References

Tables

Figures

◀

▶

◀

▶

Back

Close

Full Screen / Esc

Printer-friendly Version

Interactive Discussion

tion, and more chemical cycles, influencing the fate of pollutants and climate (McGivern et al., 2000; Saiz-Lopez and von Glasow, 2012; Simpson et al., 2015). Recent studies have identified open ocean upwelling areas in the Atlantic as large source regions for a number of brominated and iodinated oceanic trace gases (Quack et al., 2004, 2007; O'Brien et al., 2009; Raimund et al., 2011; Hepach et al., 2015a). Their sources are related to biological and chemical processes in the productive waters of the upwelling. The compounds are emitted from the ocean and are horizontally transported and vertically mixed in the marine atmospheric boundary layer (MABL) (Carpenter et al., 2010). In the Mauritanian upwelling, it was found that besides oceanic sources meteorological conditions strongly influenced the atmospheric mixing ratio of the marine compounds bromoform ( $\text{CHBr}_3$ ), dibromomethane ( $\text{CH}_2\text{Br}_2$ ) and also methyl iodide ( $\text{CH}_3\text{I}$ ) (Hepach et al., 2014). Especially the combination of a pronounced low MABL above cold upwelling waters with high concentrations and emissions of the compounds caused elevated atmospheric mixing ratios. In return, these atmospheric mixing ratios also reduce the marine emissions through a decrease of the sea–air concentration gradient (Fuhlbrügge et al., 2013). Similar relationships would be expected for other oceanic upwelling areas, where not only the oceanic emissions, but also meteorological conditions in the lowermost atmosphere, i.e., the height, type and structure of the boundary layer and trade inversion, determine the VLS contribution to atmospheric chemical processes. The intense oceanic upwelling in the Southeast Pacific off the coast of Peru transports large amounts of subsurface waters to the ocean surface and creates one of the highest productive oceanic regions worldwide (Codispoti et al., 1982). The Peruvian Upwelling is therefore a potentially intense source region for halogenated VLS, e.g. bromoform ( $\text{CHBr}_3$ ), dibromomethane ( $\text{CH}_2\text{Br}_2$ ) and methyl iodide ( $\text{CH}_3\text{I}$ ) (Yokouchi et al., 1999; Butler et al., 2007; Carpenter et al., 2009). Indeed, Schönhardt et al. (2008) detected elevated IO columns during September and November 2005 along the Peruvian coast with the SCIAMACHY satellite instrument and implied elevated iodine source gases from the Peruvian Upwelling.



## 2.1 Meteorological observations

Meteorological measurements of surface air temperature (SAT), sea surface temperature (SST), relative humidity, air pressure, wind speed and direction were taken every second at about 25 m height on R/V *METEOR* and averaged to 10 min intervals for our investigations. Atmospheric profiles of temperature, wind and humidity were obtained by 98 radiosonde launches at standard UTC time (00:00, 06:00, 12:00, 18:00 UTC) and additionally 3 hourly during the diurnal stations along the cruise track, using Vaisala RS92 radiosondes. Due to permission limitations, radiosondes could not be launched within 12 NM of the Peruvian coast. The collected radiosonde data was integrated in near real time into the Global Telecommunication System (GTS) to improve meteorological reanalysis (e.g. ERA-Interim) and operational European Centre for Medium Range Weather Forecast models (opECMWF).

## 2.2 MABL height

The radiosonde data are used to identify the height of the MABL, which is the atmospheric surface layer above the ocean in which trace gas emissions are mixed horizontally on a short time scale of an hour or less by convection and turbulence (Stull, 1988). Two different kinds of MABL can be distinguished, the convective and the stable MABL, which can be characterized by the gradient of the virtual potential temperature  $\theta_v$ . A negative or neutral gradient reveals an unstable convective layer, while a positive gradient reveals a stable atmospheric layer. In case of an increase of the virtual potential temperature from the surface, mixing in the MABL is suppressed. The upper limit of the convective MABL is set by a *stable layer*, e.g., a temperature inversion or a significant reduction in air moisture and is typically found above open ocean regions between 100 m and 3 km height (Stull, 1988; Seibert et al., 2000). For the determination of this *stable layer* above the convective MABL, we use the practical approach described in Seibert et al. (2000) and compute the virtual potential temperature during the radiosonde ascent whose increase with altitude indicates the base of a *stable layer*.

In this study the base of this *stable layer* increased by half of this *stable layer* depth is the definition for the MABL height. Over oceanic upwelling regions this stable layer can even descend to the ocean surface (e.g. Höflich et al., 1972; Fuhlbrügge et al., 2013).

### 2.2.1 Relative humidity

Estimates for atmospheric surface stability and MABL conditions in oceanic upwelling region can also be obtained from variations of the surface humidity. While the absolute humidity determines the amount of water in a specific volume of air, the relative humidity is the ratio of the partial pressure of water vapour to the equilibrium vapour pressure at the observed temperature. Variations of the SAT therefore directly influence the relative humidity at the surface. A decrease of the SAT due to cold upwelling water leads to an increase of the relative humidity, while the absolute humidity stays constant or even decreases due to condensation of water vapour once the relative humidity reaches 100 % and the air is saturated with water vapour. An elevated relative humidity in this oceanic region therefore points to stable layers with suppressed mixing of surface air and to a low and stable MABL height.

### 2.2.2 Estimation of MABL height above the upwelling

To estimate the MABL height above upwelling areas close to the coast, where radiosonde launches were permitted (Sect. 2.1) a multiple linear regression was applied. Using observed meteorological parameters revealing significant correlations (see Sect. 3.5) with the observed MABL height, relative humidity ( $x_1$ ), SAT ( $x_2$ ), SST ( $x_3$ ) and wind speed ( $x_4$ ), along the cruise we obtained the following Eq. (1):

$$\text{MABL height} = b_1x_1 + b_2x_2 + b_3x_3 + b_4x_4 \quad (1)$$

with  $b_1 = -0.0117$ ;  $b_2 = 0.0202$ ;  $b_3 = 0.0467$ ;  $b_4 = 0.0089$

## Meteorological constraints on oceanic halocarbons above the Peruvian Upwelling

S. Fuhlbrügge et al.

Title Page

Abstract

Introduction

Conclusions

References

Tables

Figures

◀

▶

◀

▶

Back

Close

Full Screen / Esc

Printer-friendly Version

Interactive Discussion



## 2.3 Atmospheric VLSL measurements

A total of 198 air samples were collected 3 hourly during the cruise at about 20 m height on the 5th superstructure deck of R/V *METEOR*. The air samples were pressurized to 2 atm in pre-cleaned stainless steel canisters with a metal bellows pump and were analyzed at the Rosenstiel School for Marine and Atmospheric Sciences (RS-MAS, Miami, Florida) within 6 months after the cruise. Details about the analysis, the instrumental precision and the preparation of the samples are described in Schauffler et al. (1999) and Fuhlbrügge et al. (2013). The atmospheric mixing ratios were calculated with a NOAA standard (SX3573) from GEOMAR.

## 2.4 Oceanic concentrations and sea–air flux

102 water samples were taken in-situ on a 3 hourly basis from the moon pool of R/V *METEOR* at a depth of 6.8 m from a continuously working water pump after 9 December 2012. The samples were then analysed for bromoform, dibromomethane and methyl iodide and other halogenated trace gases by a purge and trap system, attached to a gas chromatograph combined with an ECD (electron capture detector) with a precision of 10 % determined from duplicates. The approach is described in detail by Hepach et al. (2014).

### 2.4.1 Sea–air flux

The sea–air flux ( $F$ ) of bromoform, dibromomethane and methyl iodide is calculated with  $k_w$  as transfer coefficient and  $\Delta c$  as concentration gradient between the water and equilibrium water concentration determined from the atmospheric concentrations (Eq. 2). The transfer coefficient was determined by the air–sea gas exchange parameterization of Nightingale et al. (2000) after a Schmidt number ( $Sc$ ) correction for the

## Meteorological constraints on oceanic halocarbons above the Peruvian Upwelling

S. Fuhlbrügge et al.

Title Page

Abstract

Introduction

Conclusions

References

Tables

Figures

◀

▶

◀

▶

Back

Close

Full Screen / Esc

Printer-friendly Version

Interactive Discussion



three gases (Eq. 3).

$$F = k_w \cdot \Delta c \quad (2)$$

$$k_w = k_{\text{CO}_2} \cdot \frac{Sc^{-\frac{1}{2}}}{600} \quad (3)$$

Details on deriving the air–sea concentration gradient and emissions are further described in Hepach et al. (2014) and references therein.

## 2.5 Trajectory calculations

The Lagrangian Particle Dispersion Model FLEXPART of the Norwegian Institute for Air Research in the Department of Atmospheric and Climate Research (Stohl et al., 2005) was used to analyse the air mass origins and the transport of surface air masses along the cruise track to the free troposphere. FLEXPART has been evaluated in previous studies (Stohl et al., 1998; Stohl and Trickl, 1999). The model includes moist convection and turbulence parameterizations in the atmospheric boundary layer and free troposphere (Stohl and Thomson, 1999; Forster et al., 2007). We use the ECMWF (European Centre for Medium-Range Weather Forecasts) reanalysis product ERA-Interim (Dee et al., 2011) with a horizontal resolution of  $1^\circ \times 1^\circ$  and 60 vertical model levels as meteorological input fields, providing air temperature, horizontal and vertical winds, boundary layer height, specific humidity, as well as convective and large scale precipitation with a 6 hourly temporal resolution. Due to the spatial resolution of ERA-Interim data along the Peruvian coast defining the land–sea mask of our trajectory calculations, 98 out of 140 release points for the forward and backward trajectory calculations were analysed along the cruise track. At each these release points 10 000 forward and 50 backward trajectories were launched within  $\pm 30$  min and  $\sim 20$  m distance to the ship positions from the ocean surface. Time and position of the release events are synchronized with air samples taken on R/V *METEOR* (Sect. 2.3).



## 2.6 Oceanic contribution to MABL VSLs abundances

To obtain an estimate of the contribution of local oceanic sources to the atmospheric mixing ratios in the lowermost atmosphere above the Peruvian upwelling we apply a mass balance concept to the oceanic emissions, to the time scales of air mass transport and to the chemical loss (Fuhlbrügge et al., 2015). First we define a box above each release event with a size of  $\sim 400 \text{ m}^2$  around the measurement location and the height of the MABL and assume a steady-state observed VSLs mixing ratio within the box. During each trajectory release event we assume the specific sea–air flux to be constant and the emissions to be homogeneously mixed within the box. Then the contribution of the sea–air flux is computed as the ratio of the VSLs flux from the ocean into the MABL (in mol per day) and the total amount of VSLs in the box (in mol) and is defined as the Oceanic Delivery (OD) and OD is given in percentage per day. In addition to the delivery of oceanic VSLs to the box, the loss of VSLs out of the box into the free troposphere is defined as the CONvective Loss (COL) and is derived from the mean residence time derived from the FLEXPART trajectories in the box during each release event. Since this process is a loss process, COL is given as a negative quantity and in percentage per day. The chemical degradation of VSLs by OH and photolysis in the MABL is considered by the chemical lifetime of each compound in the MABL. We use lifetimes of 16 days for bromoform and 60 days for dibromomethane (Hossaini et al., 2010) and 3 days for methyl iodide (R. Hossaini, personal communication, 2013), representative for the tropical boundary layer. The Chemical Loss (CL) acts as loss process as well and is given as a negative quantity in percentage per day. We further assume a steady state in the box. OD, COL and CL must therefore be balanced by an advective transport of air masses in and out of the box. The change of the VSLs through advective transport is defined as Advective Delivery (AD) and given in percentage per day.

By relating OD to COL, we receive an Oceanic Delivery Ratio (ODR) (Eq. 4):

$$\text{ODR} = \frac{\text{OD} [\% \text{d}^{-1}]}{-\text{COL} [\% \text{d}^{-1}]} = \frac{\text{Sea-air flux contribution} [\% \text{d}^{-1}]}{\text{Loss of box air to the FT} [\% \text{d}^{-1}]} \quad (4)$$

Similarly, the Chemical Loss in the box (CL), respectively, the change in VSLs due to advection (AD) are related to COL to get the Chemical Loss Ratio (CLR) and the Advective Delivery Ratio (ADR) with  $\text{ADR} = 1 - \text{CLR} - \text{ODR}$ . Since CL, OD and AD are divided by  $-\text{COL}$ , ratios for source processes are positive and negative for loss processes (Fuhlbrügge et al., 2015).

### 3 Observations on R/V *METEOR*

#### 3.1 Meteorological observations

The Peruvian coast is dominated by the Southern Hemisphere trade wind regime with predominantly southeast winds (Fig. 1). The Andes, which are known to act as a barrier to zonal wind in this region, affect the horizontal air mass transport along the coast (Fig. 1b–d). The steeply sloping mountains at the coast form strong winds parallel to the South American coastline (Garreaud and Munoz, 2005), leading to distinct wind-driven oceanic upwelling of cold water along the coast. The 10-day backward trajectories reveal predominantly near-shore air masses with coastal influence and marine air masses (Fig. 1). The average wind direction observed on R/V *METEOR* during the cruise is  $160^\circ \pm 34^\circ$  (mean  $\pm \sigma$ ) with a moderate average wind speed of  $6.2 \pm 2.2 \text{ ms}^{-1}$  (Fig. 2b). ERA-Interim reveals similar winds along the cruise track with a mean wind speed of  $5.6 \pm 1.8 \text{ ms}^{-1}$  and a mean wind direction of  $168^\circ \pm 21^\circ$  (not shown here). The divergence of the wind driven Ekman transport along the Peruvian coast leads to the observed oceanic upwelling of cold waters. This upwelling is observed for several times near the coast where both, SST and SAT rapidly drop to less than  $18^\circ \text{C}$  (Fig. 2a). The impact of the cold upwelling water on the observed air masses is also visible in the

20606

## Meteorological constraints on oceanic halocarbons above the Peruvian Upwelling

S. Fuhlbrügge et al.

Title Page

Abstract

Introduction

Conclusions

References

Tables

Figures

◀

▶

◀

▶

Back

Close

Full Screen / Esc

Printer-friendly Version

Interactive Discussion





## Meteorological constraints on oceanic halocarbons above the Peruvian Upwelling

S. Fuhlbrügge et al.

Title Page

Abstract

Introduction

Conclusions

References

Tables

Figures

◀

▶

◀

▶

Back

Close

Full Screen / Esc

Printer-friendly Version

Interactive Discussion

centration ratio of dibromomethane and bromoform can be used as an indicator for the age of bromocarbon sources along the coast. Low ratios of about 0.1 have been observed and are interpreted as the emission ratios of macro algae (Yokouchi et al., 2005; Carpenter et al., 2003). The shorter mean boundary layer lifetime of bromoform (16 days) in contrast to dibromomethane (60 days) after Hossaini et al. (2010) leads to an increase of the ratio as long as the air mass is not enriched with fresh bromoform. During the cruise the concentration ratio shows a gradient from the North to the South, with a mean of  $0.44 \pm 0.07$  (Fig. 2f). Thus, we find relatively remote air masses in the North with a concentration ratio of 0.70 on 5 December and lowest ratios down to 0.31 on 24 December 2012, which implies an intensification of fresh sources towards the South that is also reflected by elevated water concentrations. Atmospheric methyl iodide along the cruise track ranges between 0.61 and 3.21 ppt with an overall elevated mean of  $1.54 \pm 0.49$  ppt generally maximizing over the oceanic upwelling regions (Fig. 2e). Correlations of methyl iodide with the bromocarbons result in  $R = 0.79$  for bromoform and  $R = 0.66$  for dibromomethane (Table 3).

Oceanic emissions during the cruise were calculated from the synchronized measurements of sea water concentrations and atmospheric mixing ratios, sea surface temperatures and wind speeds, measured on R/V *METEOR* (Sect. 2.4.1). Oceanic concentrations and atmospheric mixing ratios of each compound are weakly or not at all correlated ( $R_{\text{bromoform}} = 0.00$ ,  $R_{\text{dibromomethane}} = 0.29$  and  $R_{\text{methyl iodide}} = 0.34$ ). Mean sea–air fluxes during the cruise are  $130 \pm 554 \text{ pmol m}^{-2} \text{ h}^{-1}$  (bromoform),  $273 \pm 334 \text{ pmol m}^{-2} \text{ h}^{-1}$  (dibromomethane) and  $954 \pm 697 \text{ pmol m}^{-2} \text{ h}^{-1}$  (methyl iodide) (Fig. 2g, Table 1). The low bromocarbon emissions are probably caused by the observed elevated VLSL atmospheric concentrations, relatively low oceanic VLSL concentrations and low wind speeds and SSTs. On the other site, the high concentrations of methyl iodide in the surface waters lead to high oceanic emissions and elevated atmospheric mixing ratios. Further investigations of the distributions and sources of iodinated compounds during this cruise are carried out by Hepach et al. (2015b).

### 3.3 Lower atmosphere conditions

The atmospheric conditions in the lower troposphere, in particular the stability of the lowermost atmosphere and the height of the MABL, are obtained from radiosonde data launched along the cruise track. The relative humidity shows a strong vertical gradient at  $\sim 1$  km height (Fig. 3a). At this altitude, the relative humidity drops rapidly from over 75 % to less than 50 % which indicates a decrease in total humidity and/or an increase in air temperature due to suppressed mixing. The barrier for convective activity in this height, known as the trade inversion (Höflich, 1972), is typically found over the eastern side of tropical oceans within the lower 3 km above the surface and caused by the large-scale descending of air masses in the Hadley Cell (Riehl, 1954, 1979). This trade inversion is also reflected in the meridional wind observed by the radiosondes (Fig. 3b). Air masses below  $\sim 1$  km altitude have a strong positive meridional wind component due to the Southeast trade winds in this region, which is also visible in the forward trajectories (Fig. 1c and d). The back flow of the trade winds in the Hadley Cell to the subtropics causes a predominantly Northerly wind above  $\sim 1$  km height. The intense increase of  $\theta_v$  in combination with the relative humidity decrease and the wind shear at  $\sim 1$  km height identifies this level as a strong vertical transport barrier (Fig. 3c). However, the low SAT above the cold upwelling water creates additional stable layers below the trade inversion. In particular above the upwelling, these stable layers can reach the surface and lead to very low MABL heights, e.g., on 3, 8 or 17 December 2012 and a reduction in vertical surface air exchange. Meteorological observers on board the ship witnessed fog coinciding with the elevated relative humidity above upwelling regions lasting for almost 20 h on 15–16 December 2012, confirming the suppressed mixing within the MABL. The mean MABL height from the radiosonde observations is  $370 \pm 170$  m (ERA-Interim  $376 \pm 169$  m). Since the relative humidity, SAT, SST and wind speed are good indicators for the MABL conditions in this oceanic region and these meteorological parameters show significant correlations with the observed MABL height (Table 3), we use a multiple linear regression based



## Meteorological constraints on oceanic halocarbons above the Peruvian Upwelling

S. Fuhlbrügge et al.

Title Page

Abstract

Introduction

Conclusions

References

Tables

Figures

◀

▶

◀

▶

Back

Close

Full Screen / Esc

Printer-friendly Version

Interactive Discussion



is far less compared to observations in other source regions with high convection as in the South China and Sulu Seas (Fuhlbrügge et al., 2015). While the surface air masses can leave the MABL within hours, they are suppressed from entering the free troposphere through the trade inversion barrier. Adapting an average trade inversion height of 1.1 km as the transport barrier for surface air masses into the free troposphere reveals an average residence time of the FLEXPART trajectories of 41 h below this trade inversion height. The atmospheric VSLs below the trade inversion originate to 12 % from oceanic emissions (ODR) for bromoform, to 37 % for dibromomethane and to 103 % for methyl iodide. The increased residence time of air masses below the trade inversion, reflected by the FLEXPART trajectories, leads to a stronger enrichment of air masses with VSLs from the oceanic emissions, reflected by OD, compared to the MABL box. However, the low sea–air fluxes of bromoform and dibromomethane are by far not strong enough to lead to the observed mixing ratios. Oceanic emissions of methyl iodide could explain the atmospheric mixing ratios below the trade inversion (ODR), but the chemical degradation can destroy up to 72 % (CLR) of the observed amount within the residence time of the air masses below the trade inversion. Since the oceanic delivery is very low for the bromocarbons and the elevated oceanic delivery of methyl iodide is nearly compensated by the chemical degradation, observed VSLs abundances of all three compounds are mostly advected during the cruise, which is reflected by high ADRs within the MABL and below the trade inversion (Table 2).

### 3.5 Meteorological constrains on atmospheric VSLs in the MABL

Fuhlbrügge et al. (2013) identified the influence of meteorological conditions, in particular of MABL height variations on VSLs abundances in the tropical Northeast Atlantic above the Mauritanian Upwelling, and suggested a general correlation of MABL conditions and VSLs abundances over oceanic upwelling regions. Indeed, we also find significant high correlations between meteorological parameters and the abundances of bromoform, dibromomethane and methyl iodide (Table 3) along the Peruvian coast. The predominantly moderate winds during the cruise are negatively correlated with the

## Meteorological constraints on oceanic halocarbons above the Peruvian Upwelling

S. Fuhlbrügge et al.

Title Page

Abstract

Introduction

Conclusions

References

Tables

Figures

◀

▶

◀

▶

Back

Close

Full Screen / Esc

Printer-friendly Version

Interactive Discussion



atmospheric VSLS (bromoform  $R = -0.38$ , dibromomethane  $R = -0.53$ , and methyl iodide  $R = -0.33$ ) and positively correlated with the MABL height ( $R = 0.44$ ) implying that VSLS abundances tend to be elevated during periods of lower wind speeds, which in return lead to less mixing of surface air and therefore to lower MABL heights, in particular on 11, 15–17 and 24 December 2012. SAT and SST both correlate with atmospheric VSLS. Bromoform correlates with SAT and SST with  $R = -0.50$ , respectively  $R = -0.57$ . Correlation coefficients between methyl iodide, SAT and SST are slightly lower with  $R = -0.37$  and  $R = -0.42$ , while dibromomethane has the strongest negative correlation to SAT ( $R = -0.78$ ) and SST ( $R = -0.81$ ). Generally high correlations between a meteorological parameter and the VSLS are found for the relative humidity with  $R = 0.74$ ,  $R = 0.77$  and  $R = 0.67$  (bromoform, dibromomethane and methyl iodide). Correlation coefficients between the MABL height and the VSLS are slightly lower with  $R = -0.55$ ,  $R = -0.61$ , respectively  $R = -0.45$ . Since SAT and SST impact the MABL, which affects the relative humidity, these correlation coefficients are co-correlated with each other.

The results reveal that the MABL properties (height and character) influence the VSLS abundances at the marine surface, although not as distinct as above the Mauritanian Upwelling (Fuhlbrügge et al., 2013). A comparison between the observations from the Peruvian Upwelling and the Mauritanian Upwelling (Fig. 4) shows that the variance of the former may explain the lower correlation. Reasons for this are discussed in the following.

## 4 Discussion

The observations reveal a significant correlation between the MABL height and atmospheric VSLS abundances above the Peruvian Upwelling. However, the correlation coefficients between the determined MABL height and the atmospheric VSLS are not as high as above the Mauritanian Upwelling during the DRIVE campaign (Fuhlbrügge et al., 2013). Reasons might be the large area of the investigated region in the North-







surface and by radiosondes launched up to the stratosphere. Oceanic VSLs emissions along the cruise track were determined from air and water samples taken near the ocean surface. To investigate the transport of the observed air masses, FLEXPART forward and backward trajectories were computed.

Oceanic upwelling was observed close to the Peruvian coast by SST decreases to  $15^{\circ}\text{C}$  caused by the wind driven Ekman transport along the coast line with observed moderate wind speeds of  $6.2 \pm 2.2 \text{ ms}^{-1}$ . The oceanic upwelling coincided with elevated relative humidity including the formation of low level fog. On average a low, stable MABL height of  $307 \pm 177 \text{ m}$  was determined from radiosonde launches and multiple linear regressions during the cruise. A decrease of the MABL height from the open ocean towards the coast was observed. The radiosonde launches also revealed a distinct trade inversion at  $1.1 \pm 0.3 \text{ km}$  height. This study concentrates on the three halogenated VSLs: bromoform, dibromomethane and methyl iodide. Except for methyl iodide, oceanic emissions were low with  $130 \pm 554 \text{ pmol m}^{-2} \text{ h}^{-1}$  for bromoform,  $273 \pm 334 \text{ pmol m}^{-2} \text{ h}^{-1}$  for dibromomethane, and  $954 \pm 697 \text{ pmol m}^{-2} \text{ h}^{-1}$  for methyl iodide. Despite the low oceanic emissions, the atmospheric mixing ratios of the compounds were elevated with  $2.9 \pm 0.7 \text{ ppt}$  (bromoform),  $1.3 \pm 0.3 \text{ ppt}$  (dibromomethane) and  $1.5 \pm 0.5 \text{ ppt}$  (methyl iodide). According to our FLEXPART ERA-Interim trajectory calculations, the average residence time of surface air masses in the observed MABL was 7 h. Once these air masses left the MABL, they were suppressed in their vertical movement by the trade inversion, which was reflected by an average residence time of 41 h below the trade inversion. This additional distinct inversion layer evolved as the dominant transport barrier for MABL air into the free troposphere and led to an accumulation of air masses and the VSLs abundances therein observed during the cruise. With a simple source-loss estimate we computed the ratio between the contribution of oceanic emissions and advection to the loss of air into the free troposphere. The oceanic emissions along the cruise track explained on average only 12 % for bromoform and 37 % for dibromomethane, but 103 % for methyl iodide of the observed VSLs abundances. Considering the chemical degradation of the compounds

## Meteorological constraints on oceanic halocarbons above the Peruvian Upwelling

S. Fuhlbrügge et al.

Title Page

Abstract

Introduction

Conclusions

References

Tables

Figures

◀

▶

◀

▶

Back

Close

Full Screen / Esc

Printer-friendly Version

Interactive Discussion





---

**Meteorological constraints on oceanic halocarbons above the Peruvian Upwelling**S. Fuhlbrügge et al.

---

[Title Page](#)[Abstract](#)[Introduction](#)[Conclusions](#)[References](#)[Tables](#)[Figures](#)[◀](#)[▶](#)[◀](#)[▶](#)[Back](#)[Close](#)[Full Screen / Esc](#)[Printer-friendly Version](#)[Interactive Discussion](#)

Carpenter, L., Liss, P., and Penkett, S.: Marine organohalogens in the atmosphere over the Atlantic and Southern Oceans, *J. Geophys. Res.-Atmos.*, 108, 4256, doi:10.1029/2002JD002769, 2003.

Carpenter, L. J., Jones, C. E., Dunk, R. M., Hornsby, K. E., and Woeltjen, J.: Air-sea fluxes of biogenic bromine from the tropical and North Atlantic Ocean, *Atmos. Chem. Phys.*, 9, 1805–1816, doi:10.5194/acp-9-1805-2009, 2009.

Carpenter, L., Fleming, Z., Read, K., Lee, J., Moller, S., Hopkins, J., Purvis, R., Lewis, A., Muller, K., Heinold, B., Herrmann, H., Fomba, K., van Pinxteren, D., Muller, C., Tegen, I., Wiedensohler, A., Muller, T., Niedermeier, N., Achterberg, E., Patey, M., Kozlova, E., Heimann, M., Heard, D., Plane, J., Mahajan, A., Oetjen, H., Ingham, T., Stone, D., Whalley, L., Evans, M., Pilling, M., Leigh, R., Monks, P., Karunaharan, A., Vaughan, S., Arnold, S., Tschritter, J., Pöhler, D., Friess, U., Holla, R., Mendes, L., Lopez, H., Faria, B., Manning, A., and Wallace, D.: Seasonal characteristics of tropical marine boundary layer air measured at the Cape Verde Atmospheric Observatory, *J. Atmos. Chem.*, 67, 87–140, doi:10.1007/s10874-011-9206-1, 2010.

Codispoti, L. A., Dugdale, R. C., and Minas, H. J.: A comparison of the nutrient regimes off northwest Africa, Peru and Baja California, *Rapport et Procès-verbaux des réunions, Conseil permanent International pour l'Exploration de la Mer*, 180, 184–201, 1982.

Dix, B., Baidara, S., Bresch, J., Hall, S., Schmidt, K., Wang, S., and Volkamer, R.: Detection of iodine monoxide in the tropical free troposphere, *P. Natl. Acad. Sci. USA*, 110, 2035–2040, doi:10.1073/pnas.1212386110, 2013.

Forster, C., Stohl, A., and Seibert, P.: Parameterization of convective transport in a Lagrangian particle dispersion model and its evaluation, *J. Appl. Meteorol. Clim.*, 46, 403–422, doi:10.1175/JAM2470.1, 2007.

Fuhlbrügge, S., Krüger, K., Quack, B., Atlas, E., Hepach, H., and Ziska, F.: Impact of the marine atmospheric boundary layer conditions on VSLS abundances in the eastern tropical and subtropical North Atlantic Ocean, *Atmos. Chem. Phys.*, 13, 6345–6357, doi:10.5194/acp-13-6345-2013, 2013.

Fuhlbrügge, S., Quack, B., Tegtmeier, S., Atlas, E., Hepach, H., Shi, Q., Raimund, S., and Krüger, K.: The contribution of oceanic halocarbons to marine and free troposphere air over the tropical West Pacific, *Atmos. Chem. Phys. Discuss.*, 15, 17887–17943, doi:10.5194/acpd-15-17887-2015, 2015.

**Meteorological  
constraints on  
oceanic halocarbons  
above the Peruvian  
Upwelling**

S. Fuhlbrügge et al.

Title Page

Abstract

Introduction

Conclusions

References

Tables

Figures

◀

▶

◀

▶

Back

Close

Full Screen / Esc

Printer-friendly Version

Interactive Discussion



- Garreaud, R. and Munoz, R.: The low-level jet off the west coast of subtropical South America: structure and variability, *Mon. Weather Rev.*, 133, 2246–2261, doi:10.1175/MWR2972.1, 2005.
- Hepach, H., Quack, B., Ziska, F., Fuhlbrügge, S., Atlas, E. L., Krüger, K., Peeken, I., and Wallace, D. W. R.: Drivers of diel and regional variations of halocarbon emissions from the tropical North East Atlantic, *Atmos. Chem. Phys.*, 14, 1255–1275, doi:10.5194/acp-14-1255-2014, 2014.
- Hepach, H., Quack, B., Raimund, S., Fischer, T., Atlas, E. L., and Bracher, A.: Halocarbon emissions and sources in the equatorial Atlantic Cold Tongue, *Biogeosciences Discuss.*, 12, 5559–5608, doi:10.5194/bgd-12-5559-2015, 2015a.
- Hepach, H., Quack, B., Tegmeier, S., Engel, A., Bracher, A., Fuhlbrügge, S., Raimund, S., Lampel, J., L., G., and Krüger, K.: Contributions of biogenic halogenated compounds from the Peruvian upwelling to the tropical troposphere, in preparation, 2015b.
- Höflich, O.: The meteorological effects of cold upwelling water areas, *Geoforum*, 3, 35–46, doi:10.1016/0016-7185(72)90084-X, 1972.
- Hossaini, R., Chipperfield, M. P., Monge-Sanz, B. M., Richards, N. A. D., Atlas, E., and Blake, D. R.: Bromoform and dibromomethane in the tropics: a 3-D model study of chemistry and transport, *Atmos. Chem. Phys.*, 10, 719–735, doi:10.5194/acp-10-719-2010, 2010.
- Liu, Y., Yvon-Lewis, S., Thornton, D., Butler, J., Bianchi, T., Campbell, L., Hu, L., and Smith, R.: Spatial and temporal distributions of bromoform and dibromomethane in the Atlantic Ocean and their relationship with photosynthetic biomass, *J. Geophys. Res.-Oceans*, 118, 3950–3965, doi:10.1002/jgrc.20299, 2013.
- Mahajan, A. S., Gómez Martín, J. C., Hay, T. D., Royer, S.-J., Yvon-Lewis, S., Liu, Y., Hu, L., Prados-Roman, C., Ordóñez, C., Plane, J. M. C., and Saiz-Lopez, A.: Latitudinal distribution of reactive iodine in the Eastern Pacific and its link to open ocean sources, *Atmos. Chem. Phys.*, 12, 11609–11617, doi:10.5194/acp-12-11609-2012, 2012.
- Martin, J., Mahajan, A., Hay, T., Prados-Roman, C., Ordonez, C., MacDonald, S., Plane, J., Sorribas, M., Gil, M., Mora, J., Reyes, M., Oram, D., Leedham, E., and Saiz-Lopez, A.: Iodine chemistry in the eastern Pacific marine boundary layer, *J. Geophys. Res.-Atmos.*, 118, 887–904, doi:10.1002/jgrd.50132, 2013.
- McGivern, W., Sorkhabi, O., Suits, A., Derecskei-Kovacs, A., and North, S.: Primary and secondary processes in the photodissociation of  $\text{CHBr}_3$ , *J. Phys. Chem.-US*, 104, 10085–10091, doi:10.1021/jp0005017, 2000.

---

## Meteorological constraints on oceanic halocarbons above the Peruvian Upwelling

S. Fuhlbrügge et al.

---

Title Page

Abstract

Introduction

Conclusions

References

Tables

Figures

◀

▶

◀

▶

Back

Close

Full Screen / Esc

Printer-friendly Version

Interactive Discussion



- Nightingale, P., Malin, G., Law, C., Watson, A., Liss, P., Liddicoat, M., Boutin, J., and Upstill-Goddard, R.: In situ evaluation of air–sea gas exchange parameterizations using novel conservative and volatile tracers, *Global Biogeochem. Cy.*, 14, 373–387, doi:10.1029/1999GB900091, 2000.
- 5 O'Brien, L. M., Harris, N. R. P., Robinson, A. D., Gostlow, B., Warwick, N., Yang, X., and Pyle, J. A.: Bromocarbons in the tropical marine boundary layer at the Cape Verde Observatory – measurements and modelling, *Atmos. Chem. Phys.*, 9, 9083–9099, doi:10.5194/acp-9-9083-2009, 2009.
- Philander, G.: El-Nino and La-Nina, *Am. Sci.*, 77, 451–459, 1989.
- 10 Quack, B., Atlas, E., Petrick, G., Stroud, V., Schauffler, S., and Wallace, D.: Oceanic bromoform sources for the tropical atmosphere, *Geophys. Res. Lett.*, 31, L23S05, doi:10.1029/2004GL020597, 2004.
- Quack, B., Atlas, E., Petrick, G., and Wallace, D.: Bromoform and dibromomethane above the Mauritanian upwelling: atmospheric distributions and oceanic emissions, *J. Geophys. Res.-Atmos.*, 112, D09312, doi:10.1029/2006JD007614, 2007.
- 15 Raimund, S., Quack, B., Bozec, Y., Vernet, M., Rossi, V., Garçon, V., Morel, Y., and Morin, P.: Sources of short-lived bromocarbons in the Iberian upwelling system, *Biogeosciences*, 8, 1551–1564, doi:10.5194/bg-8-1551-2011, 2011.
- Rasmussen, R., Khalil, M., Gunawardena, R., and Hoyt, S.: Atmospheric methyl-iodide (CH<sub>3</sub>I), *J. Geophys. Res.-Oc. Atm.*, 87, 3086–3090, doi:10.1029/JC087iC04p03086, 1982.
- Riehl, H.: *Tropical Meteorology*, McGraw-Hill, New York-London, 1954.
- Riehl, H.: *Climate and Weather in the Tropics*, Academic Press, London, 1979.
- Saiz-Lopez, A. and von Glasow, R.: Reactive halogen chemistry in the troposphere, *Chem. Soc. Rev.*, 41, 6448–6472, doi:10.1039/c2cs35208g, 2012.
- 25 Saiz-Lopez, A., Lamarque, J.-F., Kinnison, D. E., Tilmes, S., Ordóñez, C., Orlando, J. J., Conley, A. J., Plane, J. M. C., Mahajan, A. S., Sousa Santos, G., Atlas, E. L., Blake, D. R., Sander, S. P., Schauffler, S., Thompson, A. M., and Brasseur, G.: Estimating the climate significance of halogen-driven ozone loss in the tropical marine troposphere, *Atmos. Chem. Phys.*, 12, 3939–3949, doi:10.5194/acp-12-3939-2012, 2012.
- 30 Schauffler, S., Atlas, E., Blake, D., Flocke, F., Lueb, R., Lee-Taylor, J., Stroud, V., and Travnicek, W.: Distributions of brominated organic compounds in the troposphere and lower stratosphere, *J. Geophys. Res.-Atmos.*, 104, 21513–21535, doi:10.1029/1999JD900197, 1999.

## Meteorological constraints on oceanic halocarbons above the Peruvian Upwelling

S. Fuhlbrügge et al.

Title Page

Abstract

Introduction

Conclusions

References

Tables

Figures

◀

▶

◀

▶

Back

Close

Full Screen / Esc

Printer-friendly Version

Interactive Discussion

Schönhardt, A., Richter, A., Wittrock, F., Kirk, H., Oetjen, H., Roscoe, H. K., and Burrows, J. P.: Observations of iodine monoxide columns from satellite, *Atmos. Chem. Phys.*, 8, 637–653, doi:10.5194/acp-8-637-2008, 2008.

Seibert, P., Beyrich, F., Gryning, S., Joffre, S., Rasmussen, A., and Tercier, P.: Review and intercomparison of operational methods for the determination of the mixing height, *Atmos. Environ.*, 34, 1001–1027, doi:10.1016/S1352-2310(99)00349-0, 2000.

Simpson, W., Brown, S., Saiz-Lopez, A., Thornton, J., and von Glasow, R.: Tropospheric halogen chemistry: sources, cycling, and impacts, *Chem. Rev.*, 4035–4062, doi:10.1021/cr5006638, 2015.

Stohl, A. and Thomson, D.: A density correction for Lagrangian particle dispersion models, *Bound.-Lay. Meteorol.*, 90, 155–167, doi:10.1023/A:1001741110696, 1999.

Stohl, A. and Trickl, T.: A textbook example of long-range transport: simultaneous observation of ozone maxima of stratospheric and North American origin in the free troposphere over Europe, *J. Geophys. Res.-Atmos.*, 104, 30445–30462, doi:10.1029/1999JD900803, 1999.

Stohl, A., Hittenberger, M., and Wotawa, G.: Validation of the Lagrangian particle dispersion model FLEXPART against large-scale tracer experiment data, *Atmos. Environ.*, 32, 4245–4264, doi:10.1016/S1352-2310(98)00184-8, 1998.

Stohl, A., Forster, C., Frank, A., Seibert, P., and Wotawa, G.: Technical note: The Lagrangian particle dispersion model FLEXPART version 6.2, *Atmos. Chem. Phys.*, 5, 2461–2474, doi:10.5194/acp-5-2461-2005, 2005.

Stull, R.: *An Introduction to Boundary Layer Meteorology*, Kluwer Academic Publishers, Dordrecht, 1988.

Yokouchi, Y., Li, H., Machida, T., Aoki, S., and Akimoto, H.: Isoprene in the marine boundary layer (southeast Asian Sea, eastern Indian Ocean, and Southern Ocean): comparison with dimethyl sulfide and bromoform, *J. Geophys. Res.-Atmos.*, 104, 8067–8076, doi:10.1029/1998JD100013, 1999.

Yokouchi, Y., Hasebe, F., Fujiwara, M., Takashima, H., Shiotani, M., Nishi, N., Kanaya, Y., Hashimoto, S., Fraser, P., Toom-Saunry, D., Mukai, H., and Nojiri, Y.: Correlations and emission ratios among bromoform, dibromochloromethane, and dibromomethane in the atmosphere, *J. Geophys. Res.-Atmos.*, 110, D23309, doi:10.1029/2005JD006303, 2005.

Yokouchi, Y., Osada, K., Wada, M., Hasebe, F., Agama, M., Murakami, R., Mukai, H., Nojiri, Y., Inuzuka, Y., Toom-Saunry, D., and Fraser, P.: Global distribution and seasonal concentra-



tion change of methyl iodide in the atmosphere, J. Geophys. Res.-Atmos., 113, D18311, doi:10.1029/2008JD009861, 2008.

Discussion Paper | Discussion Paper | Discussion Paper | Discussion Paper | Discussion Paper

**ACPD**

15, 20597–20628, 2015

**Meteorological constraints on oceanic halocarbons above the Peruvian Upwelling**

S. Fuhlbrügge et al.

Title Page

Abstract

Introduction

Conclusions

References

Tables

Figures



Back

Close

Full Screen / Esc

Printer-friendly Version

Interactive Discussion



## Meteorological constraints on oceanic halocarbons above the Peruvian Upwelling

S. Fuhlbrügge et al.

**Table 1.** Oceanic concentrations, atmospheric mixing ratios and sea–air fluxes of bromoform ( $\text{CHBr}_3$ ), dibromomethane ( $\text{CH}_2\text{Br}_2$ ), the concentration ratio of bromoform and dibromomethane and methyl iodide ( $\text{CH}_3\text{I}$ ) observed during the cruise. Values are given in mean  $\pm 1\sigma$  [range].

	$\text{CHBr}_3$	$\text{CH}_2\text{Br}_2$	$\text{CH}_2\text{Br}_2/\text{CHBr}_3$	$\text{CH}_3\text{I}$
Oceanic concentration [ $\text{pmol L}^{-1}$ ]	$6.6 \pm 5.5$ [0.2–21.5]	$4.3 \pm 3.4$ [0.2–12.7]	$0.9 \pm 0.8$ [0.1–4.2]	$9.8 \pm 6.3$ [1.1–35.4]
Atmospheric mixing ratio [ppt]	$2.9 \pm 0.7$ [1.5–5.9]	$1.3 \pm 0.3$ [0.8–2.0]	$0.4 \pm 0.1$ [0.3–0.7]	$1.5 \pm 0.5$ [0.6–3.2]
Sea–air flux [ $\text{pmol m}^{-2} \text{h}^{-1}$ ]	$130 \pm 554$ [–550–2201]	$273 \pm 334$ [–128–1321]	$0.4 \pm 8.6$ [–24.5–48.9]	$954 \pm 697$ [21–4687]

Title Page

Abstract

Introduction

Conclusions

References

Tables

Figures

◀

▶

◀

▶

Back

Close

Full Screen / Esc

Printer-friendly Version

Interactive Discussion

## Meteorological constraints on oceanic halocarbons above the Peruvian Upwelling

S. Fuhlbrügge et al.

**Table 2.** Mean  $\pm 1\sigma$  of Oceanic Delivery (OD), Advective Delivery (AD), Chemical Loss (CL), Convective Loss (COL), Oceanic Delivery Ratio (ODR), Advective Delivery Ratio (ADR) and Chemical Loss Ratio (CLR) of bromoform ( $\text{CHBr}_3$ ), dibromomethane ( $\text{CH}_2\text{Br}_2$ ) and methyl iodide ( $\text{CH}_3\text{I}$ ). Parameters have been computed for a box with the vertical extension of the MABL height (MABLH) and a mean trade inversion height of 1.1 km (TIH).

		OD [%d <sup>-1</sup> ]	AD [%d <sup>-1</sup> ]	CL [%d <sup>-1</sup> ]	COL [%d <sup>-1</sup> ]	ODR	ADR	CLR
$\text{CHBr}_3$	MABLH	10.2 $\pm$ 31.2	347.5 $\pm$ 114.3	-6.6	-341.7 $\pm$ 118.2	0.03 $\pm$ 0.09	0.99 $\pm$ 0.09	-0.02 $\pm$ 0.01
	TIH	4.4 $\pm$ 13.6	52.3 $\pm$ 24.3	-6.6	-58.5 $\pm$ 27.4	0.12 $\pm$ 0.45	1.04 $\pm$ 0.44	-0.16 $\pm$ 0.07
$\text{CH}_2\text{Br}_2$	MABLH	36.0 $\pm$ 43.5	317.0 $\pm$ 117.2	-1.8	-341.7 $\pm$ 118.2	0.11 $\pm$ 0.12	0.90 $\pm$ 0.12	-0.01 $\pm$ 0.00
	TIH	15.3 $\pm$ 18.6	36.5 $\pm$ 27.4	-1.8	-58.5 $\pm$ 27.4	0.37 $\pm$ 0.61	0.67 $\pm$ 0.61	-0.04 $\pm$ 0.02
$\text{CH}_3\text{I}$	MABLH	96.2 $\pm$ 53.7	276.2 $\pm$ 122.6	-30.7	-341.7 $\pm$ 118.2	0.31 $\pm$ 0.18	0.79 $\pm$ 0.17	-0.10 $\pm$ 0.04
	TIH	41.1 $\pm$ 23.0	39.5 $\pm$ 34.2	-30.7	-58.5 $\pm$ 27.4	1.03 $\pm$ 0.78	0.69 $\pm$ 0.66	-0.72 $\pm$ 0.31

Title Page

Abstract

Introduction

Conclusions

References

Tables

Figures

◀

▶

◀

▶

Back

Close

Full Screen / Esc

Printer-friendly Version

Interactive Discussion

## Meteorological constraints on oceanic halocarbons above the Peruvian Upwelling

S. Fuhlbrügge et al.

**Table 3.** Spearman correlation coefficients ( $R$ ) of meteorological parameters, MABL height and trade inversion height correlated with atmospheric bromoform ( $\text{CHBr}_3$ ), dibromomethane ( $\text{CH}_2\text{Br}_2$ ) and methyl iodide ( $\text{CH}_3\text{I}$ ). MABL height\* is the determined MABL height from the radiosonde launches, complimented by the regressed MABL height (Sect. 3.3). Bold coefficients have a  $p$  value of  $< 0.05$ .

	MABL height	MABL height*	Trade inversion	$\text{CHBr}_3$	$\text{CH}_2\text{Br}_2$	$\text{CH}_3\text{I}$
Wind speed	<b>0.35</b>	<b>0.44</b>	-0.06	<b>-0.38</b>	<b>-0.53</b>	<b>-0.33</b>
SAT	<b>0.65</b>	<b>0.79</b>	<b>0.24</b>	<b>-0.50</b>	<b>-0.78</b>	<b>-0.37</b>
SST	<b>0.66</b>	<b>0.80</b>	<b>0.23</b>	<b>-0.57</b>	<b>-0.81</b>	<b>-0.42</b>
SAT – SST	<b>-0.39</b>	<b>-0.47</b>	-0.11	<b>0.38</b>	<b>0.48</b>	<b>0.30</b>
Rel. humidity	<b>-0.77</b>	<b>-0.81</b>	-0.06	<b>0.74</b>	<b>0.77</b>	<b>0.67</b>
MABL height*	–	–	0.08	<b>-0.55</b>	<b>-0.61</b>	<b>-0.45</b>
$\text{CHBr}_3$	<b>-0.55</b>	<b>-0.60</b>	-0.03	–	<b>0.79</b>	<b>0.79</b>
$\text{CH}_2\text{Br}_2$	<b>-0.61</b>	<b>-0.72</b>	-0.02	<b>0.79</b>	–	<b>0.66</b>
$\text{CH}_3\text{I}$	<b>-0.45</b>	<b>-0.50</b>	<b>0.30</b>	<b>0.79</b>	<b>0.66</b>	–

Title Page

Abstract

Introduction

Conclusions

References

Tables

Figures

◀

▶

◀

▶

Back

Close

Full Screen / Esc

Printer-friendly Version

Interactive Discussion

## Meteorological constraints on oceanic halocarbons above the Peruvian Upwelling

S. Fuhlbrügge et al.

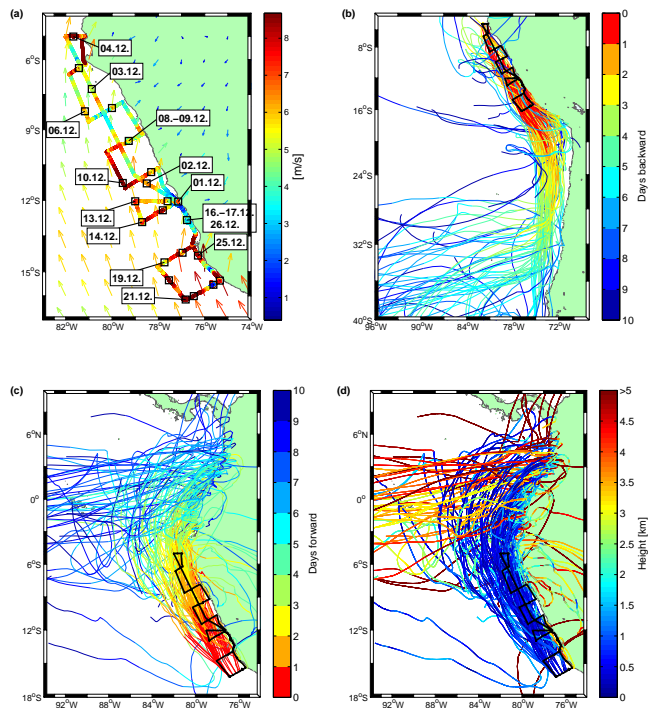


**Figure 1.** (a) 10 min mean of wind speed observed on R/V *METEOR* displayed along the cruise track; monthly mean (December 2012) of 10 m wind speed and direction from ERA-Interim displayed as arrows. (b) Extract from 10-day FLEXPART backward trajectories coloured according to the time until they reach the specific ship position on the cruise track of R/V *METEOR* (black). (c) Extract from 10-day FLEXPART forward trajectories coloured according to the time since they were released. (d) Same as (c) coloured according to the height (km) of the trajectories.

## Meteorological constraints on oceanic halocarbons above the Peruvian Upwelling

S. Fuhlbrügge et al.

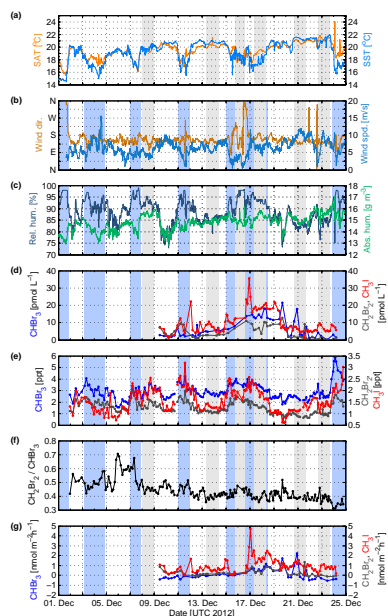


**Figure 2.** Observations during 1–25 December 2012 on R/V *METEOR*. Diurnal stations are indicated by grey background shades. **(a)** 10 min mean of the SAT (orange) and the SST (blue) in °C. According to SST decrease, upwelling regions are marked with a light blue background shade in Fig. 2b–e. **(b)** 10 min mean of wind direction in cardinal directions (ocher) and wind speed in  $\text{ms}^{-1}$  (blue). **(c)** 10 min mean of relative humidity in % (dark blue) and absolute humidity in  $\text{gm}^{-3}$  (green). **(d)** Oceanic surface concentrations of bromoform ( $\text{CHBr}_3$ , blue), dibromomethane ( $\text{CH}_2\text{Br}_2$ , dark grey) and methyl iodide ( $\text{CH}_3\text{I}$ , red) in  $\text{pmol L}^{-1}$ . **(e)** Atmospheric mixing ratios of bromoform, dibromomethane and methyl iodide in ppt. **(f)** Concentration ratio of dibromomethane and bromoform. **(g)** Sea–air flux for bromoform, dibromomethane and methyl iodide in  $\text{pmol m}^{-2} \text{h}^{-1}$ .

Title Page

Abstract

Introduction

Conclusions

References

Tables

Figures

◀

▶

◀

▶

Back

Close

Full Screen / Esc

Printer-friendly Version

Interactive Discussion

## Meteorological constraints on oceanic halocarbons above the Peruvian Upwelling

S. Fuhlbrügge et al.

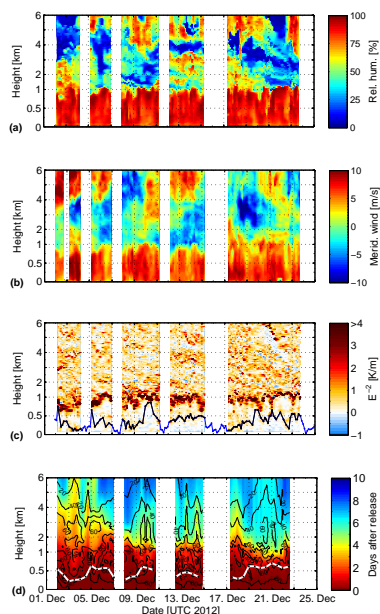


**Figure 3.** Radiosonde observations of the lower 6 km of the atmosphere between 2 and 24 December 2012 on R/V *METEOR*. Shown are (a) the relative humidity in %, (b) the meridional wind in  $\text{ms}^{-1}$  and (c) the gradient of the virtual potential temperature in  $\text{E}^{-2} \text{K m}^{-1}$  in combination with the determined MABL height (black) and the complemented MABL height above the oceanic upwelling from the multiple linear regressions (blue). (d) Distribution of 10-day FLEXPART forward trajectories. The black contour lines give the amount of trajectories in percentage that reach a specific altitude within the 10 days. The elapsed time in days until these trajectories reach this height is reflected by the colour shading. The white line shows the ERA-Interim MABL height at the ship position. Trajectory analyses gaps close to the coast are whitened (Sect. 2.5). The y axes are non-linear.

Title Page

Abstract

Introduction

Conclusions

References

Tables

Figures

◀

▶

◀

▶

Back

Close

Full Screen / Esc

Printer-friendly Version

Interactive Discussion

## Meteorological constraints on oceanic halocarbons above the Peruvian Upwelling

S. Fuhlbrügge et al.

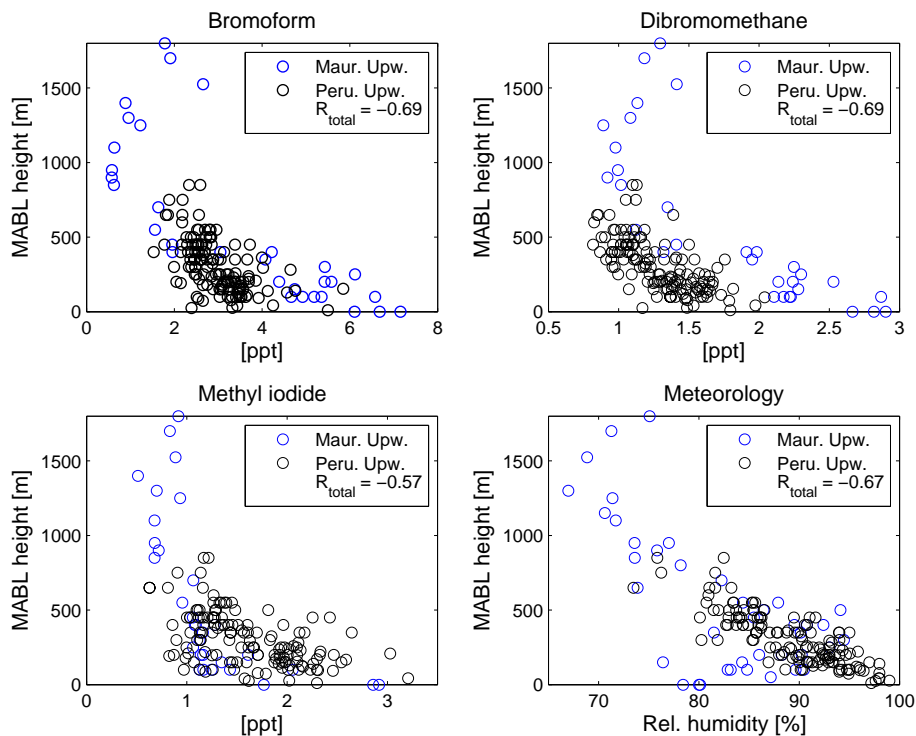


**Figure 4.** Scatter plots of atmospheric mixing ratios of bromoform, dibromomethane, methyl iodide and relative humidity vs. MABL height. Blue circles reflect observations from the Mauritanian Upwelling (Fuhlbrügge et al., 2013) and black circles from this study.  $R_{\text{total}}$  gives the Spearman correlation coefficients for both data sets together.